



Measuring instantaneous angular speed using a gear wheel as material measure to detect pitting damage during an endurance test

Yanik Koch¹ · Julian Hirschmann² · Eckhard Kirchner¹

Received: 20 March 2023 / Accepted: 20 May 2023 / Published online: 15 June 2023
© The Author(s) 2023

Abstract

Gearbox condition monitoring is mostly carried out using accelerometers at the housing. The long transfer path interferes with the information on damaged gears. Therefore, new technologies such as measuring the instantaneous angular speed (IAS) are gaining interest. But these require constructive changes in the power-transmitting elements. Therefore, this contribution uses magnetoresistive (MR) sensors and a minimally invasive integration approach to measure IAS. Three sensor classes are integrated: accelerometers at the gearbox housing, MR sensors, which use a gear wheel as a material measure and MR sensors, which use an encoder magnet at the end of the shaft. These sensor concepts are introduced by Koch et al. 2022 [1] and applied to a 3-stage bevel helical gearbox in this contribution. The first results are on artificial tooth flank damage. Therefore, this contribution focuses on real fatigue pitting damage.

A back-to-back test stand is set up for the endurance test. The tests are carried out with an overload load at a constant speed to generate fatigue pitting damage. The results are evaluated in the frequency domain by exploring the gear mesh frequency (GMF) and sidebands modulated with the shaft frequency of the damaged pinion. Results show that with all sensor concepts, the damages can be detected. Influences when using a gear wheel as a material measure are described for one measurement concept. A feature to compare the damage-specific information over the endurance test is introduced and the influence of the transfer path is evaluated through analysis of the relative rise of damage-specific amplitudes.

Messung der momentanen Winkelgeschwindigkeit mit einem Zahnrad als Maßverkörperung zur Erkennung von Pittingschäden in einem Lebensdauertest

Zusammenfassung

Die Zustandsüberwachung von Getrieben wird meist mit Beschleunigungssensoren am Gehäuse durchgeführt. Der lange Übertragungsweg beeinträchtigt die Informationen über beschädigte Zahnräder. Daher gewinnen neue Technologien wie die Messung der momentanen Winkelgeschwindigkeit (IAS) an Interesse. Diese erfordern jedoch konstruktive Änderungen an den kraftübertragenden Elementen. Daher werden in diesem Beitrag magnetoresistive (MR) Sensoren und ein minimalinvasiver Integrationsansatz zur Messung der IAS verwendet. Es werden drei Sensorklassen integriert: Beschleunigungssensoren am Getriebegehäuse, MR-Sensoren, die ein Zahnrad als Maßverkörperung nutzen und MR-Sensoren, die einen Encoder-Magneten am Ende der Welle verwenden. Diese Sensorkonzepte werden von Koch et al. 2022 [1] vorgestellt und in diesem Beitrag auf ein dreistufiges Kegelstirnradgetriebe angewendet. Die ersten Ergebnisse beziehen sich auf künstliche Zahnflankenschäden. Diese Ergebnisse werden in diesem Beitrag durch reale Pittingschäden erweitert.

✉ Yanik Koch
yanik.koch@tu-darmstadt.de

¹ Institute for product development and machine elements,
Technische Universität Darmstadt, Darmstadt, Germany

² SEW-EURODRIVE GmbH & Co KG, Bruchsal, Germany

Für den Dauerversuch wird ein Back-to-Back-Prüfstand aufgebaut. Die Versuche werden bei einer Überlastbelastung mit konstanter Drehzahl durchgeführt. Die Ergebnisse werden im Frequenzbereich ausgewertet, indem die Zahneingriffsfrequenz und die mit der Wellenfrequenz des beschädigten Ritzels modulierte Seitenbänder untersucht werden. Die Ergebnisse zeigen, dass mit allen Sensorkonzepten die Schäden erkannt werden können. Für ein Messkonzept werden Einflüsse bei der Verwendung eines Zahnrades als Maßverkörperung beschrieben. Eine Funktion zum Vergleich der schadensspezifischen Informationen über den Dauertest wird vorgestellt und der Einfluss des Übertragungsweges durch Analyse des relativen Anstiegs der schadensspezifischen Amplituden bewertet.

1 Introduction

Gearboxes are widely used to transform torque and speed in industrial plants. Unexpected faults can cause high downtime costs and early maintenance increases running costs. Therefore, the wear condition of the gearbox is monitored. In Industry state of art gear monitoring is done by using accelerometers mounted on the gearbox housing. The information on the gear condition is transferred starting at the gears meshing to the shaft, through the bearings to the housing. The vibration of the housing is measured by accelerometers and with an evaluation of the gear mesh frequency (GMF) and surrounding sidebands damages are detected [2]. Nevertheless, the elements of the transfer path interfere with the gear condition, reducing and superimposing the information reaching the accelerometers [3]. Therefore, new techniques such as measuring the instantaneous angular speed (IAS) to detect gear faults are gaining interest [4, 5]. Especially, because the high damping of the bearings is deleted from the transfer path. Mostly optical encoders measure the shaft angle. These are usually mounted at the shaft outside of the gearbox housing. This requires additional mounting at the rotating shaft and a design change. Koch et al. [1] use the gear wheel as a material measure and an encoder magnet at the shaft end with magnetoresistive (MR) sensors to measure the gear wheel angle. Using these measurement concepts no or little changes to rotating elements are required. The sensors are fixed with a bracket on the inside of the gearbox housing. It is shown in the previous work that artificial tooth flank damage can be detected in a one-stage gearbox using this measurement technique. This requires additional mounting at the rotating shaft and a design change. Therefore, Koch et al. [1] used the gear wheel as a material measure and an encoder magnet at the shaft end with magnetoresistive (MR) sensors to measure the gear wheel angle. Using these measurement concepts no or little changes to rotating elements are required. The sensors are fixed with a bracket on the inside of the gearbox housing. They showed that artificial tooth flank damage can be detected in a one-stage gearbox using this measurement technique.

To further evaluate the capability of this measurement concept for condition monitoring of gears fatigue pitting damages should be detected. Therefore, an endurance test

was carried out with a three-stage gearbox. The two sensor concepts described are integrated into the gearbox at different gear wheels and shafts, respectively. In addition, accelerometers are used as a benchmark to detect fatigue pitting damage. The endurance test was carried out for three months until the gearbox failed, because of fatigue pitting damage. This contribution presents the results focussing on the possibility to detect tooth flank damage and the influence of the transfer path.

The contribution will focus on the following research questions:

- Can fatigue pitting damage be detected using a gear wheel as a material measure or an encoder magnet to measure the IAS?
- What are the differences between the measurement concepts?
- How can sidebands around the GMF be used for damage detection?
- How does the transfer path influence the condition monitoring of gearboxes?

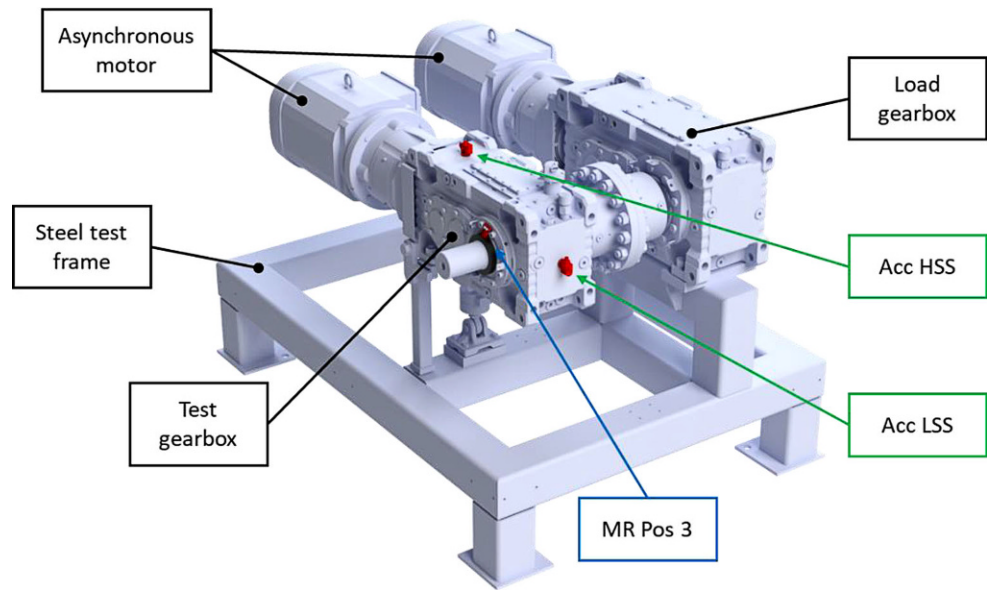
2 Method

First, the test stand and design of the endurance test are presented. Then the integrated sensors are presented. Influences on the measurement signal when using a gear wheel as the material measure is described. Finally, the data evaluation techniques used are explained.

2.1 Test stand

A 3-stage gearbox of the X series (X3KR100, SEW-Eurodrive), size 100, is being tested, see Fig. 1. The test gearbox has one bevel gear stage and two helical gear stages. The test gearbox is mounted to the steel test bench via a torque arm. A force-measuring sensor is integrated into this torque arm to monitor the torque during operation. The output shaft of the test gearbox is connected to the output shaft of the load gearbox (X series of SEW-Eurodrive, size 120) via a flange coupling. The load gearbox is bolted to the steel test bench frame. Both gearboxes are driven by asynchronous motors of the DRN series (SEW-Eurodrive)

Fig. 1 Back-to-back test stand



and controlled by frequency inverters of the MOVIDRIVE® B series (SEW-Eurodrive). During the test, the test gearbox is regulated to a constant speed of 1500rpm with a high overload to create fatigue pitting damage within 2000 operating hours.

2.2 Test design

The MR sensors used are provided by Sensitec. During the endurance test, the analogue sine and cosine signals of the MR sensors (MR Pos 3, MR Pos 4, MR Z1, MR Z3, MR B) are time-synchronous recorded with an imc CRONOSflex measuring system. The signals are sampled every 8h for a duration of 60s at 50kHz and stored locally. In addition, the HS150 IEPE acceleration sensors from Hansford are sampled with the DriveRadar® IG Edge Processing Unit from SEW-Eurodrive every 60min for a duration of 30s at 50kHz and transferred to a cloud system. An overview of the data acquisition equipment is shown in Table 1. During the endurance test, endoscopies are carried out several times to document the progress of the damage. First fatigue pitting damage is detected by an endoscopy, see Fig. 2a. After the

endurance test, the gearbox is decomposed and the damages are documented. Figure 2b shows significant fatigue pitting damage along the whole tooth flank of pinion Z4 at multiple teeth.

2.3 Sensor integration

For the description of the integrated sensors the housing of the gearbox is shown transparently in Fig. 3. The helical gear wheels are consecutively named starting at shaft A with Z1 to the damaged pinion Z4. This naming convention is also used for the GMF for further evaluations GMF Z34 is relevant, which is the meshing of the damaged pinion Z4 with the gear wheel Z3. The integrated sensors are grouped into three classes:

1. Acceleration sensors mounted onto the housing (green frame in Fig. 3)
2. Magnetostrictive sensors using a gear wheel as a material measure (blue frame in Fig. 3)
3. Magnetostrictive sensors using an encoder magnet glued to the shaft end as a material measure (orange frame in Fig. 3)

Table 1 Test stand equipment with additional information

Equipment	Information
Imc CRONOSflex	Sampling frequency: 50kHz; sampling duration: 60s; Sensors acquired: MR Pos 3, MR Pos 4, MR Z1, MR Z3, MR B, MR C
DriveRadar® IG Edge Processing Unit	Sampling frequency: 50kHz; sampling duration: 30s; Sensors acquired: Acc LSS, Acc HSS
Test gearbox X3KR100	Speed: 1500rpm; High overload
Test gearbox X3KR120	Speed: 1500rpm; No Overload

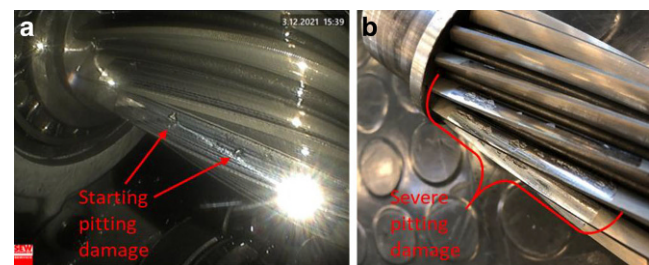
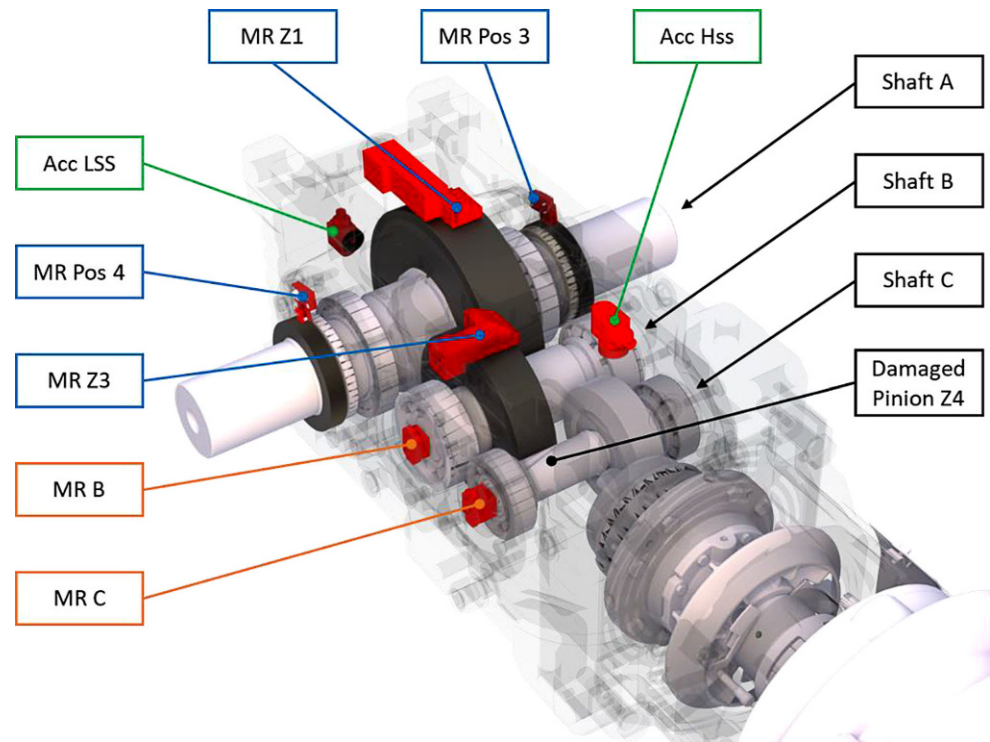


Fig. 2 Fatigue pitting damage of pinion Z4; a endoscopy during the endurance test; b after the endurance test

Fig. 3 Transparent test gearbox with integrated sensors



Two acceleration sensors are glued to the gearbox housing. One at the high-speed shaft (HSS) near shaft C, which is named Acc HSS and one at the low-speed shaft (LSS) near shaft A, which is named Acc LSS.

All MR sensors consist of two sensor elements, which acquire a sine-like wave per tooth or per revolution for the encoder magnet. The two signals of each sensor element are phase-shifted by 90° to calculate the rotation angle using the atan2-function.

The MR sensors using a gear wheel as a material measure can be further divided into MR sensors using gear wheels of the gearbox and MR sensors using additional mounted gear wheels. The MR sensors using a gear wheel of the gearbox are MR Z1 and MR Z3, they have 73 and 74 teeth, respectively. These sensors are designed by Sensitec to fit the specifications of the gear wheels. Aluminium brackets are bolted inside of the gearbox housing and the sensors are glued into 3D-printed housings of temperature-stable and oil-resistant resin. The additional mounted gear wheels have 250 teeth each and the sensor housings are bolted on the outside gearbox.

The MR sensors using an encoder magnet are MR B and MR C at shafts B and C, respectively. These are bolted into a bearing cover and sealed. Sensor MR C is not further used for evaluations because electromagnetic disturbances occurred that made the acquired signals unusable for evaluation.

2.4 Data evaluation

Figure 4 shows the two sine-like raw signals of Sensor MR Z3. Due to the phase shift of 90° one signal is called sine and the other cosine. One signal period represents one tooth of the gear wheel. The raw signal is scaled to -1 and 1 to calculate the angle φ using the atan2-function, see Eq. 1 [6]. The angle is then derived by the time to calculate the instantaneous angular speed (IAS), see Eq. 2. To evaluate the speed fluctuations caused by fatigue pitting damage a spectrum analysis is carried out using the IAS.

$$\varphi = \text{atan2}(\text{sine}, \text{cosine}) \quad (1)$$

$$\text{IAS} = \frac{\Delta\varphi}{\Delta t} \quad (2)$$

When evaluating the angle signal in Fig. 4 oscillating deviations are visible. These deviations are nearly 2 degrees. These deviations can not be explained by mechanical fluctuations of the meshing gears. The signal differs from a real sine. It has an M-W-structure, which indicates mounting deviations of the signal caused by the tooth geometry. Tooth-specific influences are shown in the first tests by Koch et al. 2022 [1]. These deviations are equal to fluctuations in the revolution speed. Therefore, influence the frequency spectrum a phase and amplitude excitation similar to the GMF, which causes a rise in the corresponding amplitudes. For

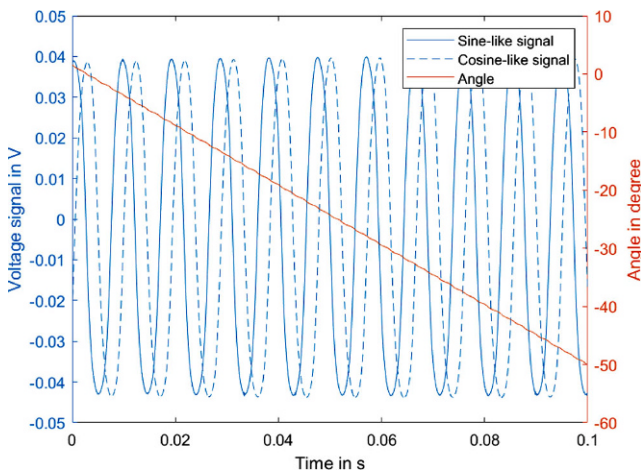


Fig. 4 Raw signal acquired with MR Z3 and calculated angle

sensor MR Z3 these are the amplitudes of GMF Z34 and its orders as well as sidebands around GMF Z34 of multiple orders. A tooth-specific influence is shown in previous tests [1]. These deviations will also influence the frequency spectrum as it is a phase and amplitude excitation by the GMF and the revolution speed. It will cause a rise in the corresponding amplitudes. For sensor MR Z3 this will be the GMF Z34 and its orders of it as well as sideband modulations around GMF Z34 of multiple orders.

2.5 Damage detection evaluating sidebands

The meshing of two gears can be described as a spring and damper with variable stiffness. Since the number of force-transmitting teeth changes periodically the coupling stiffness also changes [7]. Tolerances and manufacturing deviations result in an additional change in the coupling stiffness. This results in angular and speed fluctuations called transmission error. Deviations originate in geometrical, static and dynamic imperfections and wear of the gear meshing [8]. Faults or wear of gears cause increased amplitude and phase fluctuations of the IAS. These modulate sidebands with the rotation frequency of the damaged gear and a rise of the GMF in the frequency domain [2, 9]. Therefore, the sidebands carry damage information and will be used with the GMF to evaluate the potential of the measurement concepts for detecting fatigue pitting damage. To compare the different sensor concepts the relative rise of the amplitude is evaluated. For this, the first measurement of the endurance test defines a reference value and all subsequent amplitudes of the measurements are divided by this. This is carried out for each measurement individually and described upfront. The data analysis is conducted in Matlab® R2019b.

3 Results

For the evaluation of whether fatigue pitting damage can be detected by the presented measurement concepts and the influence of the transfer path. First, an analysis of two sensor concepts is carried out and the results are applied to the other concepts and evaluated over the endurance test. Second, the GMF and first sidebands are analysed for sensors MR Z3 and Acc HSS. Then the rise of the GMF amplitude for all sensors over the endurance test is analysed. Afterwards, a deeper look into the amplitude change of multiple sidebands is carried out for sensors MR Z3 and Acc HSS. Finally, the sum of five sidebands surrounding the GMF and the GMF is used as a feature to compare the rise for all sensors and provide a possibility to evaluate the influence of the transfer path.

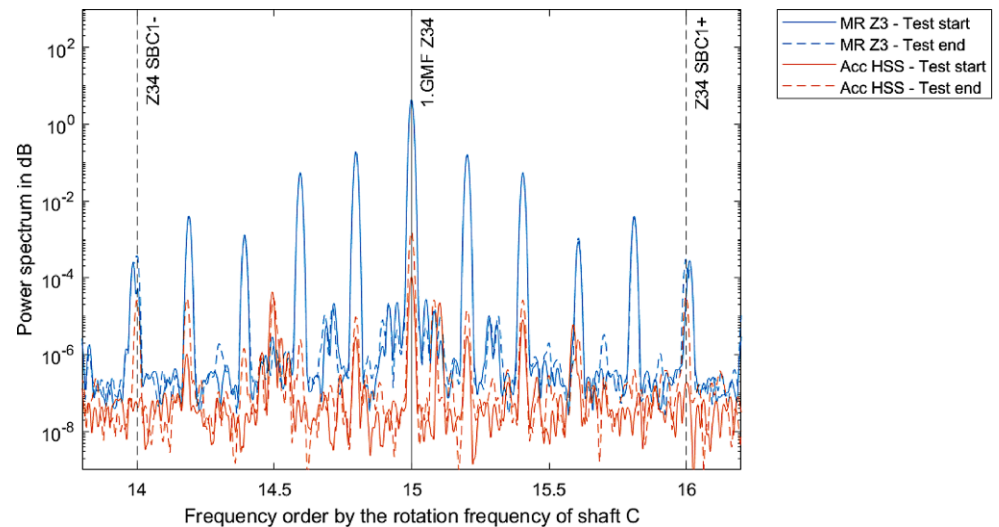
3.1 Analysis of power spectrum—gear mesh frequency first sidebands

To evaluate the change resulting from the tooth flank fatigue damage, the GMF and first sidebands of sensors MR Z3 and Acc HSS are analysed in Fig. 5 at the start and end of the endurance test. First, the power spectrum of sensor MR Z3 is analysed. The GMF does not show an increase between the start and end of the endurance test. This is caused by the high excitation of the raw signal by mounting and per tooth deviations, which superimposes the damage-dependent rise of the GMF. The rise of the GMF amplitude of sensor Acc HSS is two orders of magnitude lower than the rise of sensor MR Z3, which shows that the amplitude rise due to the damage might not be detectable at the GMF at such a high rise. Furthermore, there are high amplitudes around the GMF modulated by shaft frequency B. The first damage-relevant sideband (modulated with shaft frequency C) is near to the 5th sideband modulated by shaft frequency B and so influenced by it. But still distinguishable as the rise between the start and the end of the endurance test show. At the first sidebands, a clear rise of the amplitude from sensor Acc HSS is visible. This shows that damage can be detected with sensor Acc HSS. As there is no clear rise of the GMF for sensor MR Z3, because of the high excitation due to the measurement concept, but a rise of the first sidebands, the capabilities to detect the damage is ambiguous, when evaluating the GMF. Therefore, in the following multiple sidebands are analysed.

3.2 Relative rise of gear mesh frequency during endurance test for all sensors

The next step is to the analysis the relative rise of the GMF over the endurance test for all sensors. The tests were paused between mid-December and mid-January, which is

Fig. 5 Power spectrum of sensors MR Z3 and Acc HSS around the first order of GMF Z34 and the first sidebands



visible in the horizontal progress for this period. The amplitudes are normalised to compare the relative rise of the amplitudes. Therefore, the first value of the test is set as a reference and all amplitude values of further measurements are divided by this reference value. These values are plotted against the endurance test time in Fig. 6. As discussed above the GMF of MR Z3 does not show a rise. But all the other sensor concepts show a significant rise of the GMF amplitude relative to the reference value, which indicates that tooth flank fatigue damage can be detected with all these sensors. When looking at the MR sensors it is visible that the amplitude of MR B rises the most and the rise of MR Pos 3, MR Pos 4 and MR Z1 are similar. The longer transfer path can cause this because the damage signal is transferred from the damage at gear wheel Z4 through the meshing of Z1 and Z2 to these sensors. Furthermore, these sensors are at a shaft with a lower revolution frequency and have fewer sine-like waves per revolution, which causes

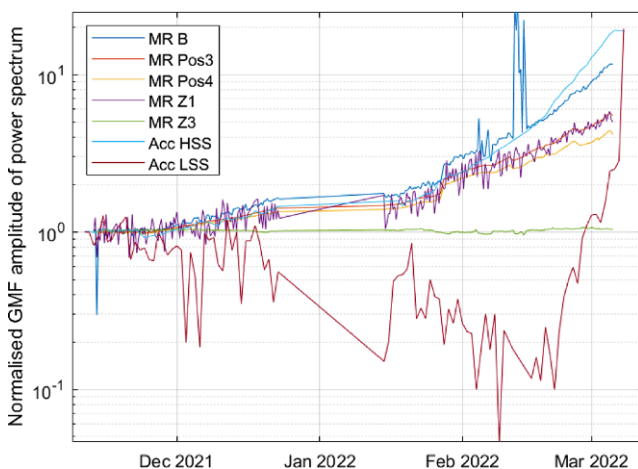


Fig. 6 Relative rise of GMF amplitude for all sensors during the endurance test

a lower accuracy. When comparing the sensors MR Pos 3 and MR Pos 4 with MR Z1 it is also visible that MR Z1 has a higher noise during the test. This can be traced back to the lower amount of teeth and the reduced accuracy of the gear wheel as the gear wheels of MR Pos 3 and MR Pos 4 are manufactured as material measure and gear wheel Z1 to transmit torque and speed. Also, similar deviations due to mounting and per tooth deviations are visible at MR Z1 as at MR Z3.

3.3 Analysis of multiple sidebands around gear mesh frequency

The sidebands, modulated by shaft frequency C of the damaged pinion, also carry information about the damage due to amplitude and phase fluctuations of the IAS. Therefore, these are further evaluated, starting with a comparison of the absolute change of five sidebands below and above the GMF Z34 between the sensors MR Z3 and Acc HSS and then all sensors are compared by merging the information of all sidebands in one feature by summing the relative change.

Figure 7 shows the plots of the five sidebands surrounding GMF Z34 modulated by the shaft frequency C. Starting at the first measurements in December 2021, it is visible that most of the amplitudes of MR Z3 are higher than the ones of Acc HSS. This is caused by the mounting and per tooth deviations described in Chapter “Data evaluation”. These effects are sensor-specific and have to be taken into account when analysing the damage dependency. The highest risen sideband amplitude is the one of SB 4 for both sensors, which shows that this effect is caused by the meshing of the gears and is not a sensor effect of MR Z3 nor Acc HSS. The amplitude values of MR Z3 are higher than for Acc HSS. This can be caused by the measuring position closer to the damage, but can also be a sensor immanent effect and has

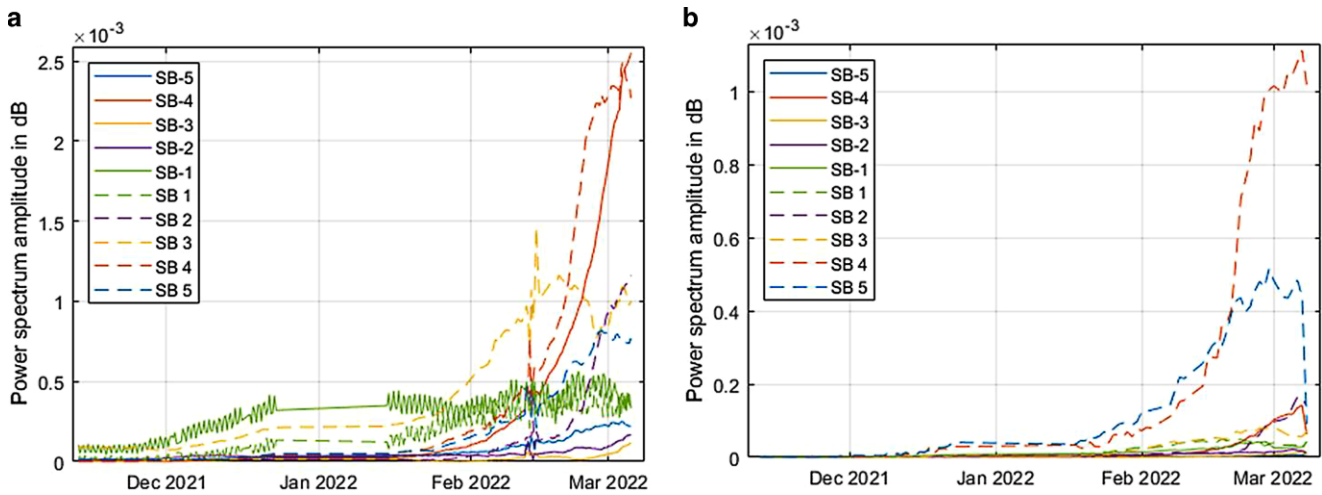


Fig. 7 Absolute rise of five sidebands below and above GMF Z34 modulated by shaft frequency C over the endurance test; **a** sensor MR Z3; **b** sensor Acc HSS

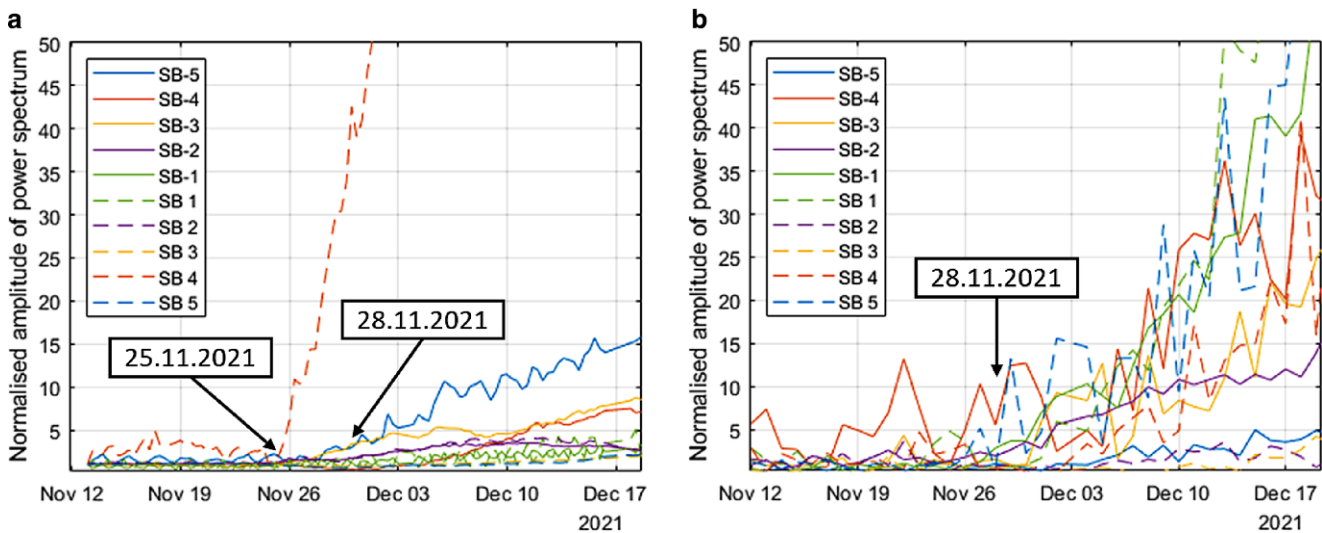


Fig. 8 Relative rise of five sidebands below and above GMF Z34 modulated by shaft frequency C at the beginning of the damage; **a** MR Z3; **b** Acc HSS

to be further evaluated in future tests. Another difference is that for MR Z3 sideband SB –4 rises nearly equal to SB 4, but for Acc HSS the rise is not that high, which could be caused by interference due to the transfer path to Acc HSS. Nevertheless, all sidebands rise during the endurance test, which shows the influence of the damage on the sidebands. However, the difference in the rise is unclear and should be focused on by future tests, so that cause and effect of the rise can be explained, what is necessary for using the sidebands for monitoring of gears.

In the next step, the beginning of the damage is analysed. For a better comparison, the relative rise of the sidebands is used for the evaluation. Therefore, the first value is set as a reference and all future values are divided by this reference value. The first rise of Sensor Z3 is at 25. November

2021, which is 2 days earlier than the first rise of Acc HSS, Fig. 8. Only one sideband rises this early and it has to be further explored and understood why this sideband rises to interpret this rise as a beginning fault. Also, the relative rise varies highly between the sidebands for MR Z3, which is also influenced by the strong modulation effects due to mounting and per tooth deviations. For Acc HSS multiple sidebands start to rise with a similar amplitude at 28. November 2021, which is a clear indicator of damage.

3.4 Relative rise of the sum of sidebands for endurance test

The GMF Z34 and five surrounding sidebands are summed up as a feature for the following evaluation. This is an ap-

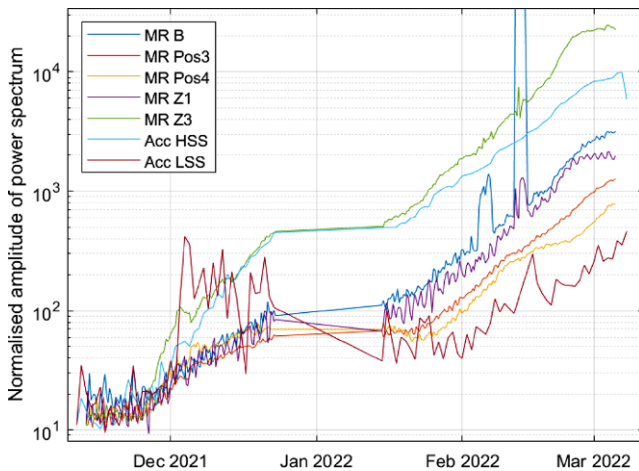


Fig. 9 Sum of normalised sideband amplitude of power spectrum for all sensors over endurance test

proach to combine the information on the damage in the sidebands and the GMF and to compare the information, which a single sensor can acquire. But, it has to be mentioned that there are a lot of influencing factors, which are not considered as the influence of the mounting and per tooth deviations. Also, the rise of these sidebands caused by speed fluctuations has to be further explored, to evaluate the observed effects. Furthermore, the Acc sensor and MR vary based on different measurement values.

Nevertheless, a clear rise in these features is visible using the data of all sensors, see Fig. 9. When looking at the MR sensors it is visible, that MR Z3 has the highest rise, followed by MR B and MR Z1, which are almost equal. This can be caused by the higher resolution of MR Z1 of 73 teeth compared to one pole per revolution for MR B. In contrast, a higher rise of MR Pos 3 and MR Pos 4 compared to MR Z1 can be expected as they have 250 teeth and are mounted at the same shaft. The evaluation of the acceleration sensors shows clearly a higher rise of Acc HSS compared to Acc LSS, which shows the influence of the transfer path. Summarised, the influence of the transfer path is visible but still superimposed due to different sensor properties.

The reliability of the feature and the capability for condition monitoring is shown by the stability of the feature value after a long standstill of the test between the end of December and the middle of January.

4 Discussion & conclusion

An endurance test was carried out producing fatigue pitting damage at a 3-stage bevel helical gearbox. To detect the damage two accelerations sensors at the housing, four MR sensors using a gear wheel as a measuring scale and one MR sensor using an encoder magnet glued to the shaft end

are used. With all sensor concepts, the damage could be detected. It was shown that mounting deviations can cause systematic measurement errors when using a gear wheel of the gearbox. These cause a high sensor-specific excitation of the sensor-specific frequencies, which equals the GMF of the used gear wheel. Still, the sidebands can be used to detect damage. But, for future tests, these deviations can be reduced by a more precise integration of the sensors and an adjustment of the MR sensors to the gear wheel. Instead of a flat sensor board, for example, a sensor board adjusted to the radius of the gear wheel can be used. Also, it is possible to reduce the influence of this disturbance by calibration of the sensor. Despite these influences, the sensor MR Z3 is the first, which shows a significant rise of one sideband. To secure these findings and to correctly interpret these results future tests have to be carried out and the rise of sidebands due to different gear damages has to be investigated. Also, the influence of the sensor concept on the sidebands has to be further investigated. Furthermore, it was shown that the transfer path influences the relative rise of damage-specific features. A longer transfer path and more signal transformations reduce the information acquired by a sensor.

In future applications, the IAS measurement has the advantage compared to acceleration measurement that the speed signal is inherited in the sensor signal. Therefore, damage detection at variable speeds using order tracking could be a research area of interest using the presented sensors. The presented endurance test was not influenced by surrounding machines and vibrations, which interfere with the measurement. The shown evaluation could further be tested in real industrial applications to explore the capabilities of condition monitoring in industrial applications.

Acknowledgements The support through Sensitec GmbH as well as the founding through the European Regional Development Fund (ERDF) is gratefully acknowledged.

Funding Open Access funding enabled and organized by Projekt DEAL.

Open Access This article is licensed under a Creative Commons Attribution 4.0 International License, which permits use, sharing, adaptation, distribution and reproduction in any medium or format, as long as you give appropriate credit to the original author(s) and the source, provide a link to the Creative Commons licence, and indicate if changes were made. The images or other third party material in this article are included in the article's Creative Commons licence, unless indicated otherwise in a credit line to the material. If material is not included in the article's Creative Commons licence and your intended use is not permitted by statutory regulation or exceeds the permitted use, you will need to obtain permission directly from the copyright holder. To view a copy of this licence, visit <http://creativecommons.org/licenses/by/4.0/>.

References

1. Koch Y, Martin G, Kirchner E, Quirnheim Pais D, Slatter R (2022) Feasibility study of measuring instantaneous angular speed of helical gears with magnetoresistive sensors. *Forsch Ingenieurwes* 86(3):451–459. <https://doi.org/10.1007/s10010-022-00590-2>
2. Randall RB (2011) *Vibration-based condition monitoring. Industrial, aerospace, and automotive applications*. Wiley, Chichester, Hoboken <https://doi.org/10.1002/9780470977668>
3. Martin G, Vogel S, Schirra T, Vorwerk-Handing G, Kirchner E (2018) Methodical evaluation of sensor positions for condition monitoring of gears. In: DS91: Proceedings of NordDesign 2018 Linköping
4. Li Y, Gu F, Harris G, Ball A, Bennett NU, Travis K (2005) The measurement of instantaneous angular speed. *Mech Syst Signal Process* 19(4):786–805. <https://doi.org/10.1016/j.ymsp.2004.04.003>
5. Li B, Zhang X, Wu J (2017) New procedure for gear fault detection and diagnosis using instantaneous angular speed. *Mech Syst Signal Process* 85:415–428. <https://doi.org/10.1016/j.ymsp.2016.08.036>
6. de Dinechin F, Istoan M (2015) Hardware implementations of fixed-point Atan2. 2015 IEEE 22nd Symposium on Computer Arithmetic. IEEE, pp 34–41 <https://doi.org/10.1109/ARITH34996.2015>
7. Tamminana VK, Kahraman A, Vijayakar S (2007) A study of the relationship between the dynamic factors and the dynamic transmission error of spur gear pairs. *J Mech Des* 129(1):75–84. <https://doi.org/10.1115/1.2359470>
8. Chin ZY, Smith WA, Borghesani P, Randall RB, Peng Z (2021) Absolute transmission error: a simple new tool for assessing gear wear. *Mech Syst Signal Process* 146(107070):1–15. <https://doi.org/10.1016/j.ymsp.2020.107070>
9. Yang X, Ding K, He G (2019) Accurate separation of amplitude-modulation and phase-modulation signal and its application to gear fault diagnosis. *J Sound Vib* 452:34–50. <https://doi.org/10.1016/j.jsv.2019.03.023>